Hindawi
Advances in Civil Engineering
Volume 2023, Article ID 9735496, 9 pages
https://doi.org/10.1155/2023/9735496

Research Article

Assessing the Quality of Concrete Tunnel Lining Exposed to Tunnel Fire through Residual Compressive Strength

Husen Alhawat, R. Hamid, Shahrizan Baharom, M. R. Azmi, and A. B. M. A. Kaish

Department of Civil Engineering, Faculty of Engineering and Built Environment, Universiti Kebangsaan Malaysia (UKM), Bangi 43600, Selangor, Malaysia

Correspondence should be addressed to R. Hamid; roszilah@ukm.edu.my

Received 5 July 2022; Revised 7 December 2022; Accepted 23 March 2023; Published 7 April 2023

Academic Editor: Md. Akter Hosen

Compressive strength performance of concrete after exposure to the elevated temperature is important for evaluating and repairing concrete structures. This paper presents an experimental study to determine the residual compressive strength of concrete used in tunnel lining after exposed to tunnel fire. Two types of concrete tunnel lining segments are evaluated in this study. One of it was constructed using a patented fire-resistant concrete (MYC) containing high volume fly ash and nanosilica (HVFANS). Another concrete tunnel lining segment was constructed using concrete containing silica fume normally used in the current construction, coded as SPC concrete. The drilled core results show that, after exposure to tunnel fire temperature up to around 1045°C, the compressive strength of MYC has dropped to 66% of the design strength. In comparison, the SPC concrete showed a decrease in compressive strength to 62% of design strength. The experimental results confirmed that the SPC segments have shown slightly lower residual compressive strength compared to the MYC segments. However, the MYC tunnel segment shows high resistance to the spalling of cover concrete compared to the SPC tunnel segment. Therefore, it can be said that the residual strength alone is not sufficient to compare the damage of concrete exposed to tunnel fire; the spalling damage observation is similarly important as it is one of the important serviceability criteria for designing concrete structures.

1. Introduction

A massive number of concrete structures have been constructed all over the world, and this number is increasing day by day. Concrete compressive strength is the main property among the mechanical and physical properties, which is necessary for the design of constructional element or determination of its load-bearing capacity. At high temperatures, the properties of hardened concrete are more complex as the physical and mechanical properties of concrete are changed, compared to those at ambient temperature. The concrete undergoes physical and chemical modifications at high temperatures, which primarily triggers mechanical changes. The free water and the bonded water evaporate when the concrete is heated at about 100–110 degree Celsius [1]. In view of the internal vapour heat conditions resulting from high heat and evaporation of the water, hydration of cement particles is improved when the temperature exceeds 300°C. As the temperature increases to 400°C, concrete hydroxide starts to decompose to calcium oxide and water [2]. As the calcium silicate hydrate (C-S-H) plays a significant role in the hardness and efficiency of the hardening process, it starts to crumble when it reaches up to 600°C [3–6].

Some researchers studied the effect of fire on the mechanical characteristics of concrete such as compressive strength, elastic modulus, and tensile strength, and the majority of them found that the mechanical characteristics decrease with the increase in temperature during a fire event [5, 7].

In the construction sector, high strength concrete (HSC) and high performance concrete (HPC) are commonly used, while silica fume [8, 9] is one of the key materials for the production of this type of concrete, because it improves the mechanical features of the concrete. Some researchers have indicated that nanosilica performs better than silica fume in improving the compressive strength of the concrete [10] while its price is identical to that of silica fume [11]. Several researchers have discovered that nanosilica particles increase the hydration of the material and effectively increase the pozzolanic activity instead of acting as a simple filler for the structure of calcium silicate hydrate which makes it denser and more compact [12, 13]. This is why nanosilica is used in high strength or performance concrete construction [14].

Previous study had shown that, at all curing periods, all samples containing nanosilica showed substantial increases in strength, where higher nanosilica contents show greater strength [15]. Nanosilica is able to increase the strength of fly ash concrete by accelerating the process of hydration [13]. After exposure to 400°C, the compressive strength of all specimens had increased, which was more effective for nanosilica-containing specimens. When the samples are heated to this temperature, the hydration process can be increased by generating dense calcium silicate hydrate by increasing nanosilica reactivity that enhances the strength properties. Exposure to 700°C leads to a significant reduction in compressive and bending strength for these specimens, primarily due to the overbuilding of vapour pressure, which led to large cracks. Furthermore, at this temperature, the binding products in the concrete paste became dehydrated causing a decrease in the strength properties. However, the residual resistance of specimens containing nanosilica was increased [13, 15]. This was primarily because of the filling effect of nanosilica and the higher content of fly ash in the specimens [15]. Additionally, 2.5% of nanosilica and 52.5% of fly ash as cement replacement were able to produce fire-resistant concrete that can retain 94% of its strength in temperatures of up to 700°C [16].

Tunnel linings can suffer heavy structural damage or even collapse when exposed to tunnel fire temperature curves. Previous studies showed that tunnel fire temperature curve is different from normal temperature curve [17, 18]. An assessment of postfire damage is the most important thing when evaluating the structural safety of a tunnel's concrete lining [17]. Wang et al. [17] studied the residual compressive strength (RCS) of small-scale lining concrete blocks and detection of inner defects in the lining structure through combined ultrasonic pulse velocity (UPV) and ultrasonic shear-wave tomography. Previous studies on concrete cube and drilled cores from small-scale slab test have reported the residual compressive strength of concrete at a maximum temperature around 700°C and compared the fire-resistant performance based on residual strength solely [8, 15, 16]. Alhawat et al. [18] studied the spalling behaviour of tunnel lining segments exposed to high temperatures. High temperature behaviour of concrete tunnel lining was also studied by Yan et al. [19, 20] through destructive testing of concrete core sample. Hua et al. [21] evaluated the spalling behaviour of concrete tunnel segment under high temperature. They proposed a simplified concrete cover spalling model based on the rate of spalling during the initiation to finishing of tunnel fire with the help of mathematical and numerical modelling. Qiao et al. [22, 23] investigated the thermomechanical damage behaviour of tunnel lining subjected to modified RABT fire loading. They utilized residual stress criterion to quantify the spalling damage depth in concrete tunnel lining. Abraham and Dérobert [24] studied the nondestructive evaluation of concrete tunnel (Mont-Blanc tunnel) after the true fire event on March 26, 1999. Ground penetrating radar and the seismic refraction method was used in their investigation. Zhai [25] also performed the nondestructive method of evaluation to quantify the damage in concrete tunnel lining after fire hazard. Most of these studies determined the residual strength of concrete through destructive or nondestructive methods, spalling mechanism, extent of spalling, and spalling rate under low-to-long-term fire events. Therefore, it can be said that both the residual strength and spalling behaviour of concrete are important to assess the condition of concrete tunnel lining after a fire event.

EFNARC [26] provides a guideline for testing of passive fire protection for concrete tunnel linings based on destructive testing of concrete core sample. Other than that, no established procedure or code provisions are available to quantify the damage and risk assessment of concrete tunnel subjected to devastating fire [20]. For realistic assessment of the fire damage of concrete tunnels, an established method would be necessary to capture the potential damage scenarios [27]. Some researchers provided emphasis on determining the residual strength and some others emphasized on spalling behaviour of cover concrete [17, 18, 20, 24, 25]. However, in reality, both parameters are important for determining the service life of the concrete tunnel after a fire event. Therefore, this study is conducted to understand the relationship between these two factors for assessing the fire damage of tunnel lining made of two different types of concrete.

2. Experimental Method

2.1. Materials. Materials and mix design proportions for MYC and SPC tunnel lining segments are shown in Tables 1 and 2.

2.2. Testing Setup for Attaining Tunnel Fire Temperature. To attain tunnel fire temperature to study its effect on the concrete tunnel linings, an innovative testing setup is designed and described by Alhawat et al. [18]. Two rings of tunnel lining were constructed, one using MYC and the other using SPC. Figure 1(a) shows the typical arrangement of tunnel lining segments to form the tunnel ring and Figure 1(b) shows the assembling process during the construction of tunnel ring. Brick walls with opening are constructed covering the both tunnel rings to provide confinement effect. This helped to achieve the desired tunnel fire time-temperature curve of RABT-ZTV [18].

All the details for the test and the temperature measurement during the test were described in the previous study [18]. Figures 2(a) and 2(b) show the peak fire and maximum temperatures during the test measured by a thermal image camera. The time temperature curves for this test compared with the RABT-ZTV car is shown in Figure 3.

Table 1: Physical properties of the materials and mix design proportion for MYC (reinforced concrete segments using HVFANS concrete, Malaysian patent code MY-163281-A) (18).

Material	Proportion	Type (class)	Specific gravity	Size	Weight (kg/m^3)
Fly ash	52.5%	F	2.1	—	278
Nano silica	2.5%	Cembinder 8	—	—	26.56
Portland cement	45%	Type 1	—	—	225.8
Polypropylene fibre	1%	—	0.9	Length 12 mm	1
Coarse aggregate	—	—	2.07	Max. 10 mm	942.6
Fine aggregate	—	—	2.75	Max. 4.75	682.01
Water	0.34 (W/C)	Normal tap water	—		154.85
Superplasticizer	0.4–2%	Darex super 20	—		5.31

Table 2: Physical properties of the materials and mix design proportion for SPC.

Material	Proportion (%)	Type (class)	Specific gravity	Size
Cement including fly ash	90	Fly ash type F	2.1	—
Silica fume	10	—	—	—
Polypropylene fibre	1	—	0.9	Length 12 mm

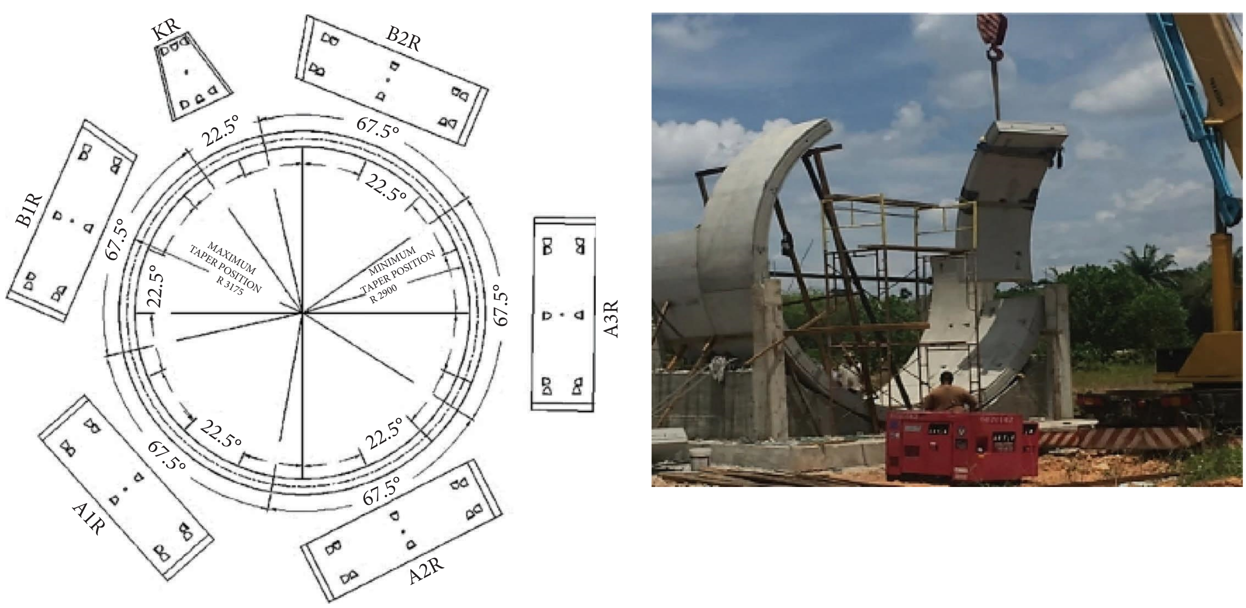

(a) (b)

Figure 1: (a) Elevation of the ring and (b) assembling the segments into rings (18).

2.3. Drilling and Coring Method. After the fire test, concrete cores with a diameter of 100 mm were drilled in the entire 275 mm depth of the MYC and SPC full-scale segments to determine their residual compressive strength. All the drilled concrete cores were obtained according to the standard procedures [28, 29]. In the SPC and MYC segments, the reinforcing steel was mapped before obtaining the concrete core with the intent of preventing the extraction of the rebar in the recovered cores. Drilled cores were extracted and sealed in plastic bags. These cores were transported to the lab for further tests. The length of the cores was further adjusted at both ends to be approximately 200 mm to meet the standard guidelines [29, 30].

Core drilling was performed in different locations depending on the spalling area on the segments for both types of concrete tunnels, considering the drilling locations to be representing the damaged areas as shown in Figure 4. Six cores were drilled in this study from the segments for both types of concrete tunnels according to the standard procedure [31].

Core samples were extracted from the structural portion of the tunnel using core drilling equipment that has diamond bits added to the drilling barrel. Since any movement could lead to a spoiled core during the drilling process, the rig was securely fixed to the concrete segment. To prevent cutting out a twisted core, the rig was set up perpendicular to

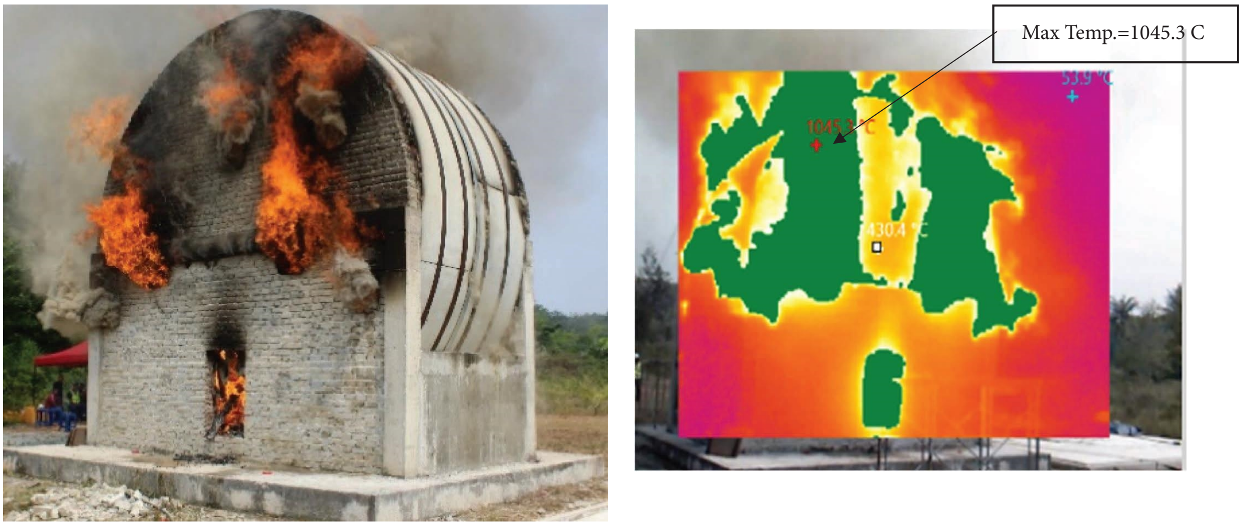

Figure 2: The tunnel ring fire test (a) during the peak fire at 15 minutes and (b) infrared photos for maximum temperature.

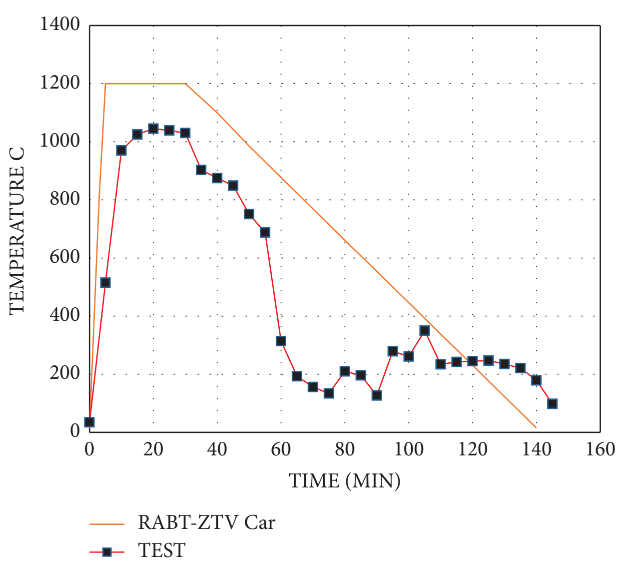

Figure 3: Time-temperature curves produced by test setup and the RABT-ZTV.

the surface on which the core would be extracted. Figure 5 shows the core drilling process in the full-scale tunnel segment, and Figure 6 shows the core samples after being extracted from the tunnel segments.

In the laboratory, the drilled cores were visually tested to verify their state and to investigate their condition to better interpret the cores' compressive strength. All core specimens were prepared by grinding their ends to obtain appropriate length, smooth ends, and perpendicular shape to the longitudinal core axis before measuring the compression strength [29].

3. Experimental Results

The concrete cores were tested to use these values in the measurement of L/D ratio and to conform to the criteria for the cross-sectional area of the core compression test [32]. For compliance, both ends of the cores were shortened to approximately 200 mm. Thus, the diameter to height ratio is equal to ½; thus, there is no need to apply any factors to reduce the obtained value [30]. The core compressive strength is calculated dividing the peak load by the core cross-sectional area depending on the average core diameter [29].

The compressive strengths of MYC and SPC concrete segments before and after exposure to the elevated temperature are presented in Table 3. The compressive strength before heating was obtained using cubes. Thus, there is a need to make adjustment to cylinder compressive test value (f_c) equivalent to the cube compressive test values (f_{cu}). Therefore, to gain the f_{cu} after heating, the formula $f_c = 0.8\, f_{cu}$ was used, as referred in the standard guidelines [33]. The percentage of residual compressive strength was calculated using the following equation:

$$\text{residual compressive strength (\%)} = \frac{f_c\,(\text{before exposure to heating})}{f_c\,(\text{after exposure to heating})} \times 100. \quad (1)$$

The test results indicated that for tunnel fire temperature, compressive strength had reduced greatly for both types of concrete mix. The MYC tunnel concrete showed a little bit higher residual strength. The strength of MYC concrete

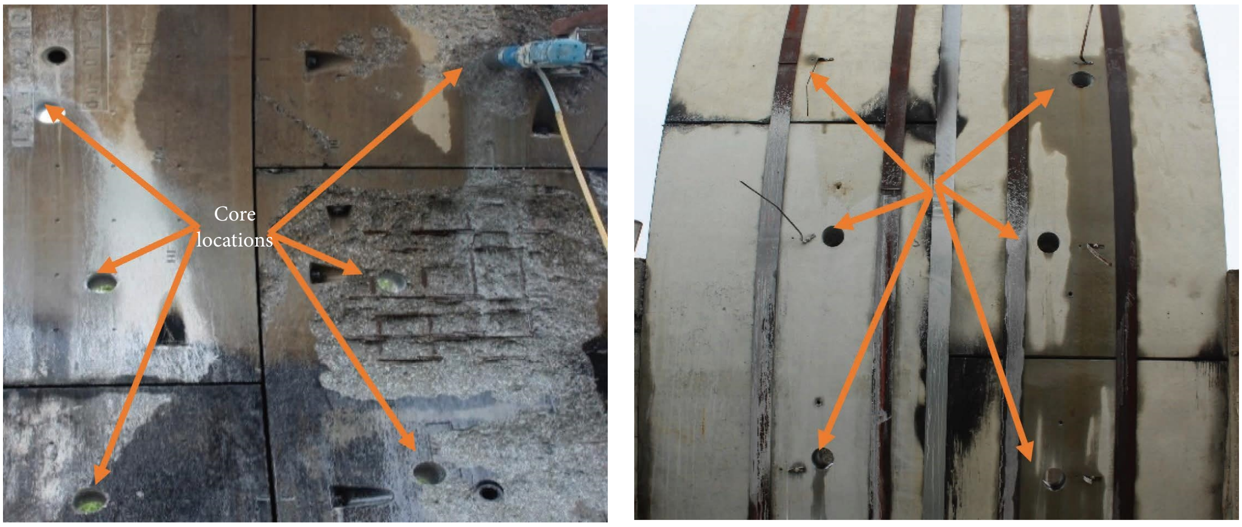

(a) (b)

Figure 4: Coring drill locations in the full-scale segments for MYC and SPC concrete tunnels; (a) inner surface view and (b) outer surface view.

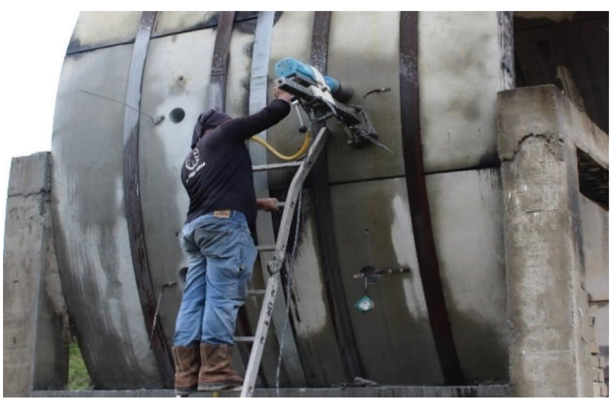

Figure 5: Drilling cores in the full-scale segments for MYC and SPC concrete.

Figure 6: Extracted core samples from the tunnel segments.

decreased and remained at 66.04% after exposure to an elevated temperature of 1000°C and above, whereas the SPC concrete strength was decreased to 62.46% after exposure to tunnel fire.

Therefore, the residual compressive strength of MYC concrete was reduced and dropped to 48 MPa, which meant it was reduced by 33.96% after exposure to a 1000°C tunnel fire. Figure 7 shows the comparison of the residual compressive strengths between MYC and SPC concrete.

This reduction in strength was due to more vapour pressure and more cracks than when the concrete was exposed to 700°C and above, which affected the strength of concrete. The elevated temperature also affected the cement paste binder. These results were also compared with the results obtained by a previous researcher [34]. It was noticed that there difference in the compressive strength between both types of concrete was not large, although there was significant difference in spalling behaviour between them. Such differences are because the components for MYC concrete have more resistance to spalling and fire than on the compressive strength and static loading. The MYC concrete's behaviour after exposure to temperature up to 1000°C can be reflected by both pozzolanic and filler influences of NS in the mixture, which enhanced the concrete microstructure and increased the content of calcium silica hydrate.

Figure 8 shows the failure of the SPC and MYC core samples after compression test. From the fire test, it can be seen that explosive spalling occurred mostly in the SPC tunnel lining as shown in Figure 9. Moreover, some of the concrete covers had been scalded off, exposing the steel reinforcements, which greatly influence the load-bearing performance of the tunnel linings. However, in both concrete mixes, the PP fibre had melted due to the very high temperatures, reducing the amount of pore pressure build-up [35]. Spalling contours show how much damage has been occurred in a particular point, as well as how much of the surface area has been damaged. Spalling patterns for SPC and MYC segments are depicted in Figures 9 and 10. Some patterned cracks were appeared in one of the MYC

Table 3: Compressive strength of the MYC and SPC concrete segments.

Samples	Before exposure to fire, f'_{cu} (MPa)	After exposure to fire of higher than 1000°C			
		f_c' (MPa)	f'_{cu} (MPa)	Residual compressive strength (%)	Average residual strength (%)
MYC 1	72.30	37.3	46.63	64.5	
MYC 2	72.30	38.4	48	66.39	66.04
MYC 3	72.30	38.9	48.63	67.25	
SPC 1	72.45	36.37	45.46	62.75	
SPC 2	72.45	34.5	43.13	59.53	62.46
SPC 3	72.45	37.75	47.19	65.1	

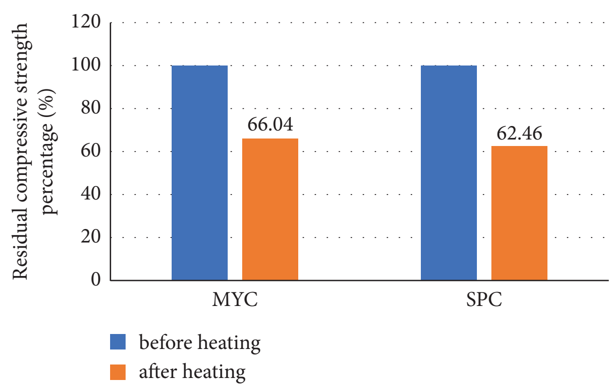

Figure 7: Comparison of residual compressive strengths between MYC and SPC concrete.

Figure 8: Failure of coring SPC and MYC sample after compression.

segments, but the ring itself showed no signs of spalling as shown in Figures 9 and 10. The SPC segments displayed a variety of severe spalling patterns and had exposed the reinforcing steel that could have weakened the structure. Spalling patterns are random and not related to the boundary conditions.

The volume of spalling was used to calculate the depths of the spalling. Each segment's spalled area was measured and converted to a percentage. Segments BR1, AR1, AR3, BR2, and KR have a spalling rate of 45.36%, 40.7%, 36.84%, 49.16%, and 7.92%, respectively, in the SPC tunnel segments. On the other hand, segments BR1, AR1, AR3, BR2, and KR had spalling volumes of 1.65%, 4.76%, 4.88%, 7.15%, and 0.283%, respectively, in the MYC tunnel segment. Cracking in the MYC segments was analysed by. However, visual inspection shows that 16.56% of the MYC segments had cracked due to high temperature exposure.

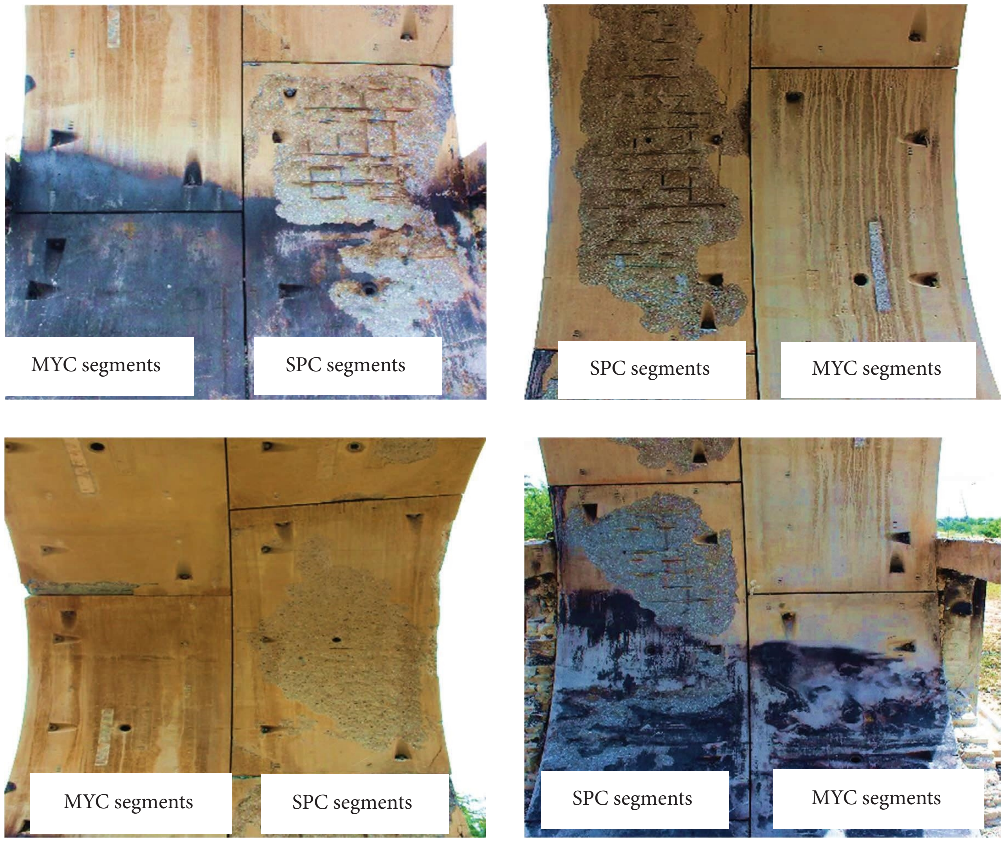

Figure 9: Spalling at different locations of SPC and MYC segments.

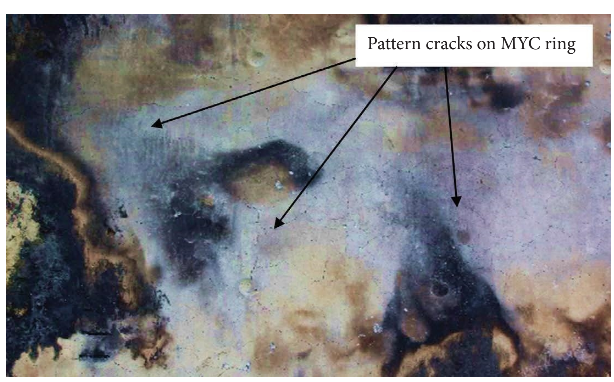

Figure 10: Cracking on the MYC segment.

4. Discussion

The experimental outcome of this study showed that the spalling was totally different on the SPC segments and MYC segments. Severe spalling occurred in the SPC segments, whereas there was no spalling in the MYC segments. This might be due to the presence of silica fume in the SPC that reduced the permeability and thus increased the vapour pressure during the fire leading to more spalling occurrence. However, the design strengths for MYC and SPC were the same. The residual strengths after fire exposure were almost the same at different locations on the tunnel rings. Therefore, it is difficult to judge the health of fire exposed concrete tunnel only based on the design and residual strengths of concrete.

For a concrete structure, satisfying the serviceability requirements is as necessary as satisfying the strength requirements. Even though historic events rarely observed a tunnel failure due to a fire event [21, 36], severe damage in terms of spalling was observed in such events. Therefore, serviceability requirement in terms of concrete spalling is an important criterion for assessing the health of a concrete tunnel. Characterizing concrete spalling in terms of the spalling starting time is also important to understand the degradation pace of the tunnel concrete in a fire event. Hua et al. [21] mentioned that the spalling normally starts when gas temperature inside the tunnel lining reaches the spalling starting temperature. However, spalling starting times for MYC and SPC segments were not being able to be determined in this study as the tunnel was closed from both ends as shown in Figure 2. Furthermore, depth of spalling together with the area of spalling plays a vital role to understand the depth of damage in the tunnel lining [36]. This also helps to understand the condition of reinforcing steels inside the tunnel lining.

5. Conclusion

The main objective of this study was to assess the health of concrete tunnel lining after exposed to tunnel fire. Based on the experimental results, the following conclusions are drawn:

(i) The findings revealed that, after exposed to high temperature, the compressive strength of MYC concrete tunnel lining dropped to 66.04% of design strength, whereas the conventional concrete for the current construction of tunnels (SPC concrete) decreased to 62.46% of design strength.

(ii) It is also observed that the spalling of SPC segments was severe where the reinforcing steel also exposed in most of the SPG segments that could have weakened the tunnel structure. However, the MYC segments only show the patterned surface cracking, even though the residual strengths of both types of concrete were almost the same after exposure to the standard fire.

This concludes that determining the performance of different types of concrete tunnel lining with different material components drilled cores is not enough to know the after fire health of a concrete tunnel. Spalling behaviour including the spalling rate and depth of spalling are also important to assess the health of the tunnel lining. A particular mix design may produce good concrete in terms of the residual strength; however, surface spalling may cause severe damage resulting in failure to meet the serviceability requirement of the tunnel structure. Therefore, this study concludes that the residual strength of concrete spalling behaviour should be evaluated to assess the condition of fire-exposed concrete tunnel lining.

Data Availability

The datasets used in this study are available from the authors upon request.

Conflicts of Interest

The authors declare that they have no conflicts of interest.

Acknowledgments

The authors acknowledge the financial contribution of the Ministry of Higher Learning through project nos. DIP-2019-002 and PRGS/2/2015/TK08/UKM/02/1. The authors also acknowledge the financial, technical, and expertise contribution of the UKM industry and government body collaborators (SPC Industries Sdn. Bhd. and Fire and Rescue Department, Malaysia).

References

[1] J. Geng, Q. Sun, W. Zhang, and C. Lü, "Effect of high temperature on mechanical and acoustic emission properties of calcareous-aggregate concrete," *Applied Thermal Engineering*, vol. 106, pp. 1200–1208, 2016.

[2] M. Li, C. X. Qian, and W. Sun, "Mechanical properties of high-strength concrete after fire," *Cement and Concrete Research*, vol. 34, no. 6, pp. 1001–1005, 2004.

[3] J. P. Ingham, "Application of petrographic examination techniques to the assessment of fire-damaged concrete and masonry structures," *Materials Characterization*, vol. 60, no. 7, pp. 700–709, 2009.

[4] B. Georgali and P. E. Tsakiridis, "Microstructure of fire-damaged concrete. A case study," *Cement and Concrete Composites*, vol. 27, no. 2, pp. 255–259, 2005.

[5] W. Zheng, H. Li, and Y. Wang, "Compressive behaviour of hybrid fiber-reinforced reactive powder concrete after high temperature," *Materials and Design*, vol. 41, pp. 403–409, 2012.

[6] B. Zhang, "Effects of moisture evaporation (weight loss) on fracture properties of high performance concrete subjected to high temperatures," *Fire Safety Journal*, vol. 46, no. 8, pp. 543–549, 2011.

[7] R. Felicetti, "The drilling resistance test for the assessment of fire damaged concrete," *Cement and Concrete Composites*, vol. 28, no. 4, pp. 321–329, 2006.

[8] R. K. Ibrahim, R. Hamid, and M. R. Taha, "Strength and microstructure of mortar containing nanosilica at high temperature," *ACI Materials Journal*, vol. 111, no. 2, pp. 163–170, 2014.

[9] Z. Li, H. Wang, S. He, Y. Lu, and M. Wang, "Investigations on the preparation and mechanical properties of the nano-alumina reinforced cement composite," *Materials Letters*, vol. 60, no. 3, pp. 356–359, 2006.

[10] Y. Qing, Z. Zenan, K. Deyu, and C. Rongshen, "Influence of nano-SiO2 addition on properties of hardened cement paste as compared with silica fume," *Construction and Building Materials*, vol. 21, no. 3, pp. 539–545, 2007.

[11] U. Skarp, R. Troli, R. T. M. Collepardi, and S. Collepardi, "Optimization of silica fume, fly ash and amorphous nano-silica in superplasticized high-performance concretes," *Optimization*, vol. 221, 2004.

[12] T. Ji, "Preliminary study on the water permeability and microstructure of concrete incorporating nano-SiO2," *Cement and Concrete Research*, vol. 35, no. 10, pp. 1943–1947, 2005.

[13] J. J. Gaitero, I. Campillo, and A. Guerrero, "Reduction of the calcium leaching rate of cement paste by addition of silica nanoparticles," *Cement and Concrete Research*, vol. 38, no. 8-9, pp. 1112–1118, 2008.

[14] J. Vera-Agullo, D. Portillo-Rico, M. J. García-Casas, A. Gutiérrez-Martínez, J. M. Mieres-Royo, and J. Grávalos-Moreno, "Mortar and concrete reinforced with nano-materials," *Nanotechnology in Construction 3*, pp. 383–388, Springer, Berlin, Germany, 2009.

[15] R. K. Ibrahim, R. Hamid, and M. R. Taha, "Fire resistance of high-volume fly ash mortars with nanosilica addition," *Construction and Building Materials*, vol. 36, pp. 779–786, 2012.

[16] R. K. Ibrahim, *The strength and micro structures of sustainable high strength high-volume fly ash concrete with nano materials exposed to high temperature*, Ph.D. thesis, UKM, Kuala Lumpur, Malaysia, 2013.
[17] Q. Wang, D. Chen, K. Zhu et al., "Evaluation residual compressive strength of tunnel lining concrete structure after fire damage based on ultrasonic pulse velocity and shear-wave tomography," *Processes*, vol. 10, no. 3, p. 560, 2022.
[18] H. Alhawat, R. Hamid, S. Baharom, M. R. Azmi, and A. B. M. A. Kaish, "Thermal behaviour of unloaded concrete tunnel lining through an innovative large-scale tunnel fire experimental testing setup," *Construction and Building Materials*, vol. 283, Article ID 122718, 2021.
[19] Z. G. Yan, H. H. Zhu, J. Woody Ju, and W. Q. Ding, "Full-scale fire tests of RC metro shield TBM tunnel linings," *Construction and Building Materials*, vol. 36, pp. 484–494, 2012.
[20] Z. G. Yan, H. H. Zhu, and J. W. Ju, "Behavior of reinforced concrete and steel fiber reinforced concrete shield TBM tunnel linings exposed to high temperatures," *Construction and Building Materials*, vol. 38, pp. 610–618, 2013.
[21] N. Hua, A. Tessari, and N. Elhami Khorasani, "Characterizing damage to a concrete liner during a tunnel fire," *Tunnelling and Underground Space Technology*, vol. 109, Article ID 103761, 2021.
[22] R. J. Qiao, Z. S. Shao, F. Liu, and W. Wei, "Damage evolution and safety assessment of tunnel lining subjected to long-duration fire," *Tunnelling and Underground Space Technology*, vol. 83, pp. 354–363, 2019.
[23] R. J. Qiao, Z. S. Shao, W. Wei, and Y. Y. Zhang, "Theoretical investigation into the thermo-mechanical behaviours of tunnel lining during RABT fire development," *Arabian Journal for Science and Engineering*, vol. 44, no. 5, pp. 4807–4818, 2018.
[24] O. Abraham and X. Dérobert, "Non-destructive testing of fired tunnel walls: the Mont-Blanc Tunnel case study," *NDT and E International*, vol. 36, no. 6, pp. 411–418, 2003.
[25] Z. T. Zhai, "Ultrasonic testing and experimental study on damage of lining structure concrete after tunnel fire," M.Sc. thesis, China Jiliang University, Hangzhou, China, 2020.
[26] Efnarc, *Guidelines for Testing of Passive Fire protection for concrete Tunnels Linings*, European federation dedicated to specialist construction chemicals and concrete systems, Brussels, Belgium, 2006.
[27] F. Souza, M. Rosignuolo, S. Andreini, C. La Mendola, and Knaust, "Probabilistic thermo-mechanical analysis of a concrete tunnel lining subject to fire," in *Proceedings of the IFireSS 2017–2nd International Fire Safety Symposium*, pp. 997–1004, Naples, Italy, June 2017.
[28] Aci Committee 214, *214 4R-03 Guide for Obtaining Cores and Interpreting Compressive Strength Results*, ACI, Toronto, Ontario, 2003.
[29] M. F. A. Alwash, "Assessment of concrete strength in existing structures using nondestructive tests and cores: analysis of current methodology and recommendations for more reliable assessment," L'Université De Bordeaux, Bordeaux, France, Docteur De, 2017.
[30] AMST, "C 42/C 42M – 04 Obtaining and testing drilled cores and sawed beams of concrete 1," *Practice*, vol. 23, no. 11, pp. 4–8, 2001.
[31] J. H. Bungey and S. G. Millard, *Testing of Concrete in Structures*, Taylor and Francis, Milton Park, UK, 1995.
[32] Astm C39, "Standard test method for compressive strength of cylindrical concrete specimens: C39/C39m-18," *Am. Soc. Test. Mater*, vol. 4, p. 8, 2018.
[33] M. H. Mussa, A. A. Mutalib, R. Hamid, and S. N. Raman, "Dynamic properties of high volume fly ash nanosilica (HVFANS) concrete subjected to combined effect of high strain rate and temperature," *Latin American Journal of Solids and Structures*, vol. 15, no. 1, pp. 1–19, 2018.
[34] Bs En 206-1, "Concrete - Part 1: specification, performance, production and conformity," *Eurocode*, vol. 3, pp. 1–72, 2000.
[35] M. Saeidpour and L. Wadsö, "Moisture equilibrium of cement based materials containing slag or silica fume and exposed to repeated sorption cycles," *Cement and Concrete Research*, vol. 69, pp. 88–95, 2015.
[36] N. Hua, A. Tessari, and N. Elhami Khorasani, "Quantifying uncertainties in the temperature-time evolution of railway tunnel fires," *Fire Technology*, vol. 57, no. 1, pp. 361–392, 2020.